Proceedings of the ASME 2010 3rd Joint US-European Fluids Engineering Summer Meeting and 8th International Conference on Nanochannels, Microchannels, and Minichannels
FEDSM-ICNMM2010
August 1-5, 2010, Montreal, Canada

FEDSM-ICNMM2010-30304

AN EXPERIMENT STUDY OF WALL SLOT JETS PERTINENT TO TRAILING EDGE COOLING OF TURBINE BLADES

Zifeng Yang, Anand Gopa Kumar, Hirofumi Igarashi and Hui Hu (✉)
Department of Aerospace Engineering
Iowa State University, Ames, IA 50011
Email: huhui@iastate.edu

ABSTRACT

An experimental study was conducted to quantify the flow characteristics of wall jets pertinent to trailing edge cooling of turbine blades. A high-resolution stereoscopic PIV system was used to conduct detailed flow field measurements to quantitatively visualize the evolution of the unsteady vortex and turbulent flow structures in cooling wall jet streams and to quantify the dynamic mixing process between the cooling wall jet streams and the main stream flows. The detailed flow field measurements are correlated with the adiabatic cooling effectiveness maps measured by using pressure sensitive paint (PSP) technique to elucidate underlying physics in order to improve cooling effectiveness to protect the critical portions of turbine blades from the harsh ambient conditions.

INTRODUCTION

Thermodynamic analysis reveals that thermal efficiency and power output of a gas turbine can be increased greatly with higher turbine inlet temperatures. Modern gas turbines are operating at peak turbine inlet temperature well beyond the maximum endurable temperature of the turbine blade material. As a result, hot gas-contacting turbine blades have to be cooled intensively by using various techniques, such as internal convective cooling and film cooling on the blade exterior, in order to increase the fatigue lifetime of the turbine blades. One of the most difficult regions to cool is the blade's trailing edges, due to geometric constraints in combination with aerodynamic demands. From an aerodynamic point of view the trailing edge should be designed as thin as possible in order to reduce aerodynamic losses. This conflicts with the blade structural integrity and cooling design requirements as enough coolant cannot be channeled into the thin trailing edges. It has been found that most of the catastrophic failures for turbine blades commonly originate at the edges – trailing edges, tips and roots. Common modes of failure are cracking, erosion, or simply melting. Oddly enough, even though trailing edge failure will reduce the service time between maintenance, and severely restrict operating temperatures, trailing edge cooling has received little attention from the research community. In this study, we particularly concerned with the trailing edge cooling of turbine blades.

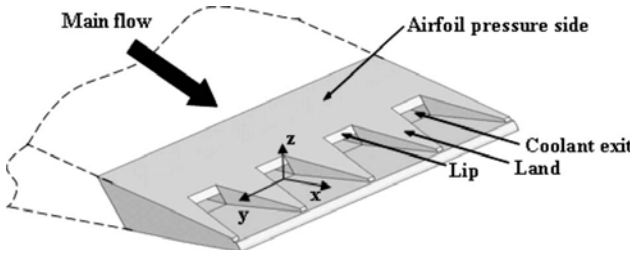

Fig. 1: Trailing edge cooling slots at pressure side beakout.

The trailing edges of modern high pressure turbine blades are usually cooled by jets blown tangentially through a breakout slot on the pressure-side of the blade, which is shown schematically in Fig. 1. Overheating is a consequence of failure of these cooling streams to protect the blade surface from hot free-stream gas. At a basic level, the hot gas gets mixed to the surface, overheating the blades. Holloway et al. [1, 2] found

that trailing edge cooling is not as effective as anticipated: hot gas reaches the surface more readily than expected. For instance, numerical simulations based on steady, Reynolds-averaged analysis approaches predict notably better cooling effectiveness than the measured values obtained in the experiments done for blade design. More recently, numerical simulations of Medic & Durbin [3] have revealed that three-dimensional unsteadiness, which occurs in cooling slot jets, could be a primary cause of poor trailing edge protection. This suggests a potential path to re-designing the coolant streams to alleviate the heat load. While Medic & Durbin [3] showed that cooling jet streams contain unsteady, three-dimensional vortical components that have a large effect on transporting heat and contaminants to the surface due to the coherent, three-dimensional vortex shedding from the upper lip of the breakout slot, the computational evidence has not been verified yet experimentally.

While several experimental investigations have been conducted in recent years to investigate trailing edge cooling of turbine blades, the majority of those previous studies were conducted mainly based on the pressure loss measurements and the quantification of adiabatic cooling effectiveness on the wall downstream the breakout of cooling wall jet streams (see Taslim et al. [4], Brundage et al. [5]; Cakan&Taslim [6]; Choi et al. [7]). Very few experimental studies (Matini et al. [8]) can be found in the literature to quantify the details of the flow characteristics of cooling wall jets in the cutback regions.

In present study, an experimental investigation was conducted to quantify the flow characteristics of the wall jets pertinent to the trailing edge cooling of turbine blades. A high-resolution Stereoscopic Particle Image Velocimetry (PIV) system was used to conduct detailed flow field measurements to quantitatively visualize the evolution of the unsteady vortex and turbulent flow structures in the cooling jet streams and to quantify the dynamic mixing process between the cooling jet streams and the main stream flows. Based on mass transfer analogy theory, pressure sensitive paint (PSP) was used to measure the adiabatic cooling effectiveness distribution on the protected surface in the trailing edge region. The detailed flow field measurements are correlated with the adiabatic cooling effectiveness measurements to elucidate underlying physics in order to explore new trailing edge cooling strategy for improving cooling effectiveness to protect the critical portions of turbine blades from the harsh ambient conditions.

EXPERIMENTAL SETUP

The experiments were conducted in a small open-circuit wind tunnel located in the Department of Aerospace Engineering at Iowa State University. The tunnel has a test section with an 8 inch × 5 inch (i.e., 200mm×125 mm) cross section. The walls of the test section are optically transparent. The tunnel has a contraction section upstream of the test section with honeycombs and screen structures installed ahead of the contraction section to provide uniform low-turbulence incoming flow into the test section. The turbulence intensity at the inlet of the test section was found to be less than 1.0% measured by using a hotwire manometer.

Figure 2 shows the pictures of the experimental rig and the test model used in the present study. The trailing edge of a turbine blade is simplified as a combination of two plates with six land structures to form five slot jets flowing tangentially along the surface of the lower plate. As shown in the Fig. 2(b), the lower surface of the trailing edge breakout model is coated with oxygen sensitive paint for the adiabatic film cooling effectiveness measurements. While air flow from the small wind tunnel was supplied to simulate the hot main stream, the cooling channel is fed by pure nitrogen to simulate the cooling jet streams to protect the surface on the lower plate. The mixing of the hot ambient gas into the cooling flow is simulated by the mixing of ambient air flow into the nitrogen jet streams.

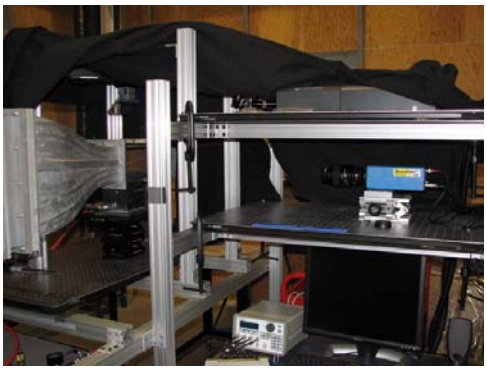

(a). Experimental rig

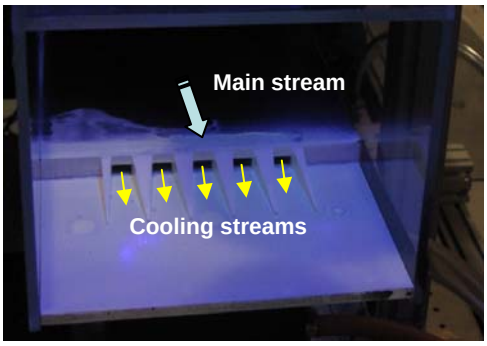

(b). Test model of the trialing edge breakout

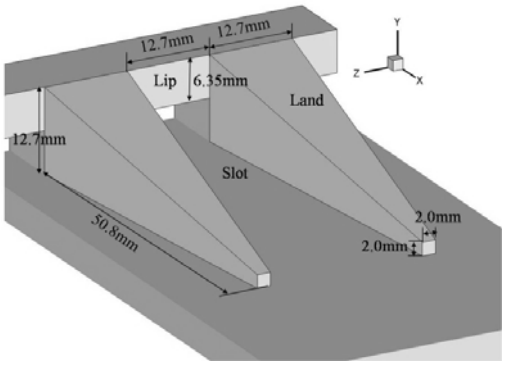

(c). the dimension of the test model

Fig. 2: The experimental rig and the test model

In the present study, the main flow velocity at the inlet of the test section was set as U_∞ = 16.2 m/s. Based on the length of the trailing edge film cooling model, the corresponding Reynolds number is 3.15×10^5. In the present study, the experimental study was conducted with five different blowing ratios, which is defined as the velocity ratio between the cooling jet stream and main stream (i.e., $M = U_{cooling\ stream}/U_{main\ stream}$), between 0 and 1.6. The corresponding Reynolds number of the cooling slot jets, Re_c is in the range of 3,000 to 11,000 based on the slot height *H*.

A high-resolution stereoscopic PIV system was in the present study to conduct detailed flow field measurements in the cutback region downstream the breakout slots of the trailing edge model. For the PIV measurements, the main air stream and the cooling nitrogen jet streams were seeded with ~ 1 μm oil droplets by using droplet generators. Illumination was provided by a double-pulsed Nd:YAG laser (NewWave Gemini 200) adjusted on the second harmonic and emitting two pulses of 200 mJ at the wavelength of 532 nm with a repetition rate of 10 Hz. The laser beam was shaped to a sheet by a set of mirrors, spherical and cylindrical lenses. The thickness of the laser sheet in the measurement region is about 1.0mm. The illuminating laser sheet was first aligned along the main stream flow direction to conduct PIV measurements in the X-Y planes. Then, the laser sheet was rotated 90 degrees to illuminate flow structures in the cross planes normal to the main stream flow direction to conduct Stereo PIV measurements in the Y-Z planes at different locations downstream of the slot exits.

For the Stereo PIV measurements in the Y-Z planes, two high resolution 14-bit CCD cameras (PCO1600, Cooke Corp.) were used for the PIV image acquisitions. The two cameras were arranged in an angular displacement configuration to get a large overlapped view. With the installation of tilt-axis mounts, laser illumination plane, the lenses and camera bodies were adjusted to satisfy the Scheimpflug condition. The CCD cameras and the double-pulsed Nd:YAG lasers were connected to a workstation (host computer) via a Digital Delay Generator (Berkeley Nucleonics, Model 565), which controlled the timing of the laser illumination and the image acquisition. A general in-situ calibration procedure was conducted to obtain the mapping functions between the image planes and object planes for the stereoscopic PIV measurements. A target plate (~ 150mm ×150 mm) with 500-μm-diameter dots spaced at intervals of 2 mm was used for the in-situ calibration. The mapping function used in the present study was a multi-dimensional polynomial function, which is fourth order for the directions parallel to the laser illumination plane (i.e., X and Y directions), and second order for the direction normal to the laser sheet plane (i.e., (Z direction). The coefficients of the multidimensional polynomial were determined from the calibration images by using a least-square method. For the PIV image processing, instantaneous PIV velocity vectors were obtained by a frame to frame cross-correlation technique involving successive frames of patterns of particle images in an interrogation window 32×32 pixels. An effective overlap of 50% of the interrogation windows was employed in PIV image processing. For the stereo PIV measurements, with the mapping functions obtained by the in-situ calibration procedure, the two-dimensional displacements in the two image planes are used to reconstruct all three components of the velocity vectors in the laser illumination planes (i.e., Y-Z planes). After the instantaneous velocity vectors (u_i, v_i, w_i) were determined, instantaneous vorticity (ω_z) could be derived. The time-averaged quantities such as mean velocity (*U, V, W*), ensemble-averaged vorticity, turbulent velocity fluctuations ($\overline{u'}, \overline{v'}, \overline{w'}$) and normalized turbulent kinetic energy ($TKE = \frac{1}{2U_\infty^2}(\overline{u'u'} + \overline{v'v'} + \overline{w'w'})$) distributions were obtained from a cinema sequence of 500 frames of instantaneous velocity fields.

Following the work of Han and his co-workers [9-10], pressure sensitive paint (PSP) was used to measure the adiabatic film cooling effectiveness in the present study with the theory of the mass transfer analogy. As shown in Fig 2(b), the surface of the lower plate was coated with Binary UniCoat oxygen sensitive paint. A UV light stroke at the wavelength of 400nm was used to excite the sensor molecules pre-mixed in the oxygen sensitive paint. A CCD camera (PCO. 1600) with a 610nm filter was used to acquire the photoluminescence image of the oxygen sensitive paint. During the experiments, the surface temperature of lower plate was also measured by using a thermocouple probe for the compensation of the temperature effects on the measurement results through a post-processing procedure. Further information about the Stereo PIV and PSP techniques, experimental rig setup and test model, and measurement uncertainty analysis is available at Yang [11].

RESULTS AND DISCUSSIONS

A. PIV MEASUREMENT RESULTS IN THE MID-PLANES OF THE COOLING JET STREAMS

PIV measurement results in the mid-plane of the cooling jet streams were given in Fig. 3 and Fig.4 with the lands between the cooling slot jets removed. From the measured typical instantaneous velocity distribution at the blow ratio of M=0.43 given in Fig. 3, it can be seen clearly that the cooling jet stream would form a buffer layer between the protected surface on the lower plate and the mainstream air flow until X/H=4.0 downstream (i.e., about 4 times of the slot height H, H=6.35mm) after the exit of cooling slots. A similar phenomenon was also found at blow ratios of 0.37 and 0.47 by Caken and Taslim [6]. At further downstream, the cooling stream was found to mix with the main stream intensively to generate a mixed turbulent boundary layer. The shearing effect generated by the differences of momentum between slot and mainstream flow triggered mixing turbulent flow between the flows. Fig. 3(b) shows the instantaneous vorticity distribution for the same condition as above. Apparently, paired-vortex was generated in the region between the slot and main flow with adverse sign of the vorticity value. While it can be predicted that a two-dimensional geometry will produce a Von Karman vortex street, it is far from obvious in the instantaneous vorticity field. It has been interpreted by Medic and Durbin [3]

that the three-dimensionality can suppress coherent shedding. The negative value of vorticity found near the bottom wall is generated by boundary layer flow. Fig. 3(d) shows the ensemble-averaged turbulent kinetic energy distribution. The low T.K.E region after the breakout until X/H ≈ 3 supports the finding about the length of the buffer layer between slot flow and bottom wall. The high T.K.E region observed after X/H=4.5 in Fig. 3(d) may indicate that the fully developed turbulent flow enhances the mixing process.

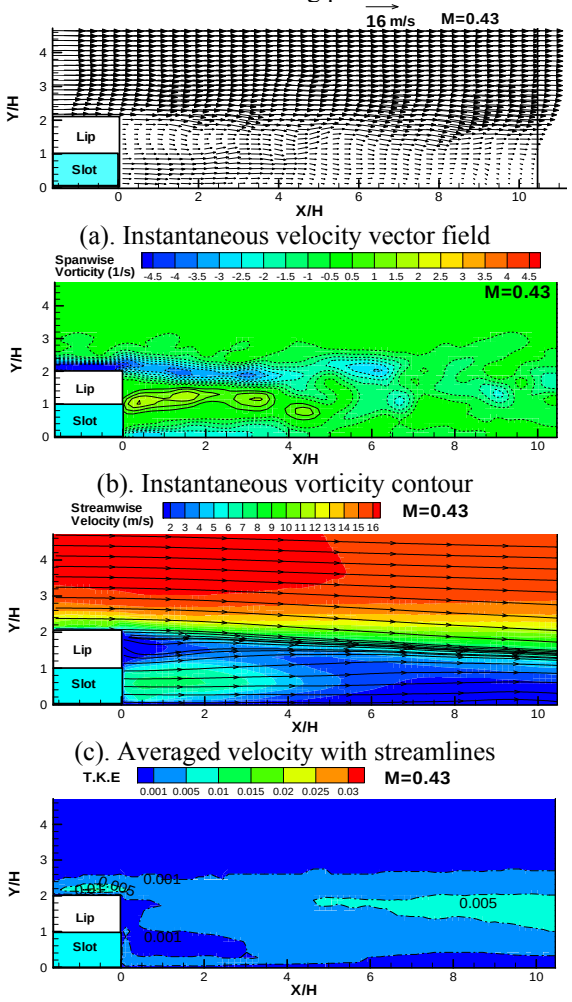

(a). Instantaneous velocity vector field

(b). Instantaneous vorticity contour

(c). Averaged velocity with streamlines

(d). Averaged turbulent kinetic energy

Fig. 3: PIV measurement results at blow ratio of M = 0.43.

Figure 4(a-d) shows the PIV measurement results for blow ratio M=1.6. At a high blow ratio, on one hand the slot is filled more and more with laminar or transitional slot flow and this behavior prevents effective entrainment of the mainstream flow into the slot jet flow. It also induces the buffer boundary layer of the slot flow to extend to X/H=8, which can be observed from the instantaneous vorticity field and averaged T.K.E field in Fig. 4. On the other hand, the mix layer at high blow ratio triggers the mainstream flow entrainment into the slot valley more easily. This flow pattern is different from the observation at low blow ratios. At low blow ratios, the streamlines before X/H=4 are observed to tilt upward for M=0.43 because of the less flow momentum of the slot flow. Due to the effect of momentum difference, the downward slope of the streamlines of main flow starting from the lip end is much larger at M=1.6 than the one at M=0.43.

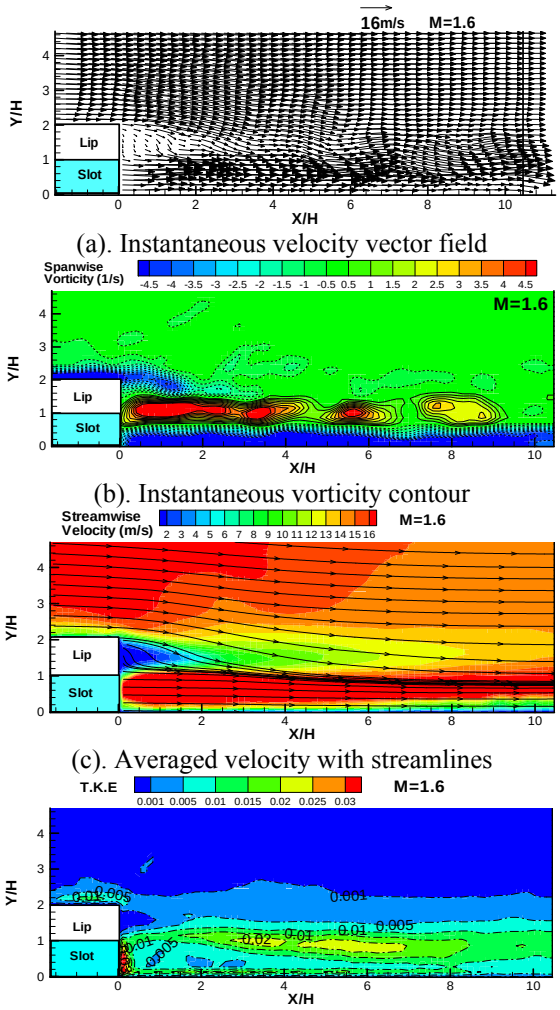

(a). Instantaneous velocity vector field

(b). Instantaneous vorticity contour

(c). Averaged velocity with streamlines

(d). Averaged turbulent kinetic energy

Fig. 4: PIV measurement results at blow ratio of M =1.6.

The effect of blow ratios on the X-component velocity at different distances downstream of the slot exit is shown in the velocity profiles in Fig. 5. There was negative velocity under Y/H=1.5 for M=0 because the mainstream flow will generate a circulation region when passing the lip end. The velocity profiles do not vary much in the near wall region between X/H=0.5 to X/H=2, which indicates that the slot flow remains laminar in this region. In the region between X/H=2 to X/H=4, the slot flow still keeps a laminar jet shape, but the difference between the velocity in the laminar region (Y/H=0~1) and mixing region (Y/H=1~2) is below 1.5m/s for M=0.43, which means the mixing process is almost fully developed. The slot flow further decelerates and the flow accelerates in the mixing region at X/H=8. The mainstream flow decelerates a little as well due to the mixing. At X/H=8, the profiles tend to be monotonically increased curves for blow ratios less than 1, which indicates the combined flow has been developed to a

turbulent boundary layer flow. Even though the relatively simple flow pattern in the mid-span plane, to some extent, could be related to explain the cooling effectiveness on the bottom surface, it must be emphasized that it is definitely not enough to reveal the flow characteristics because of the three-dimensional unsteady flow feature [3].

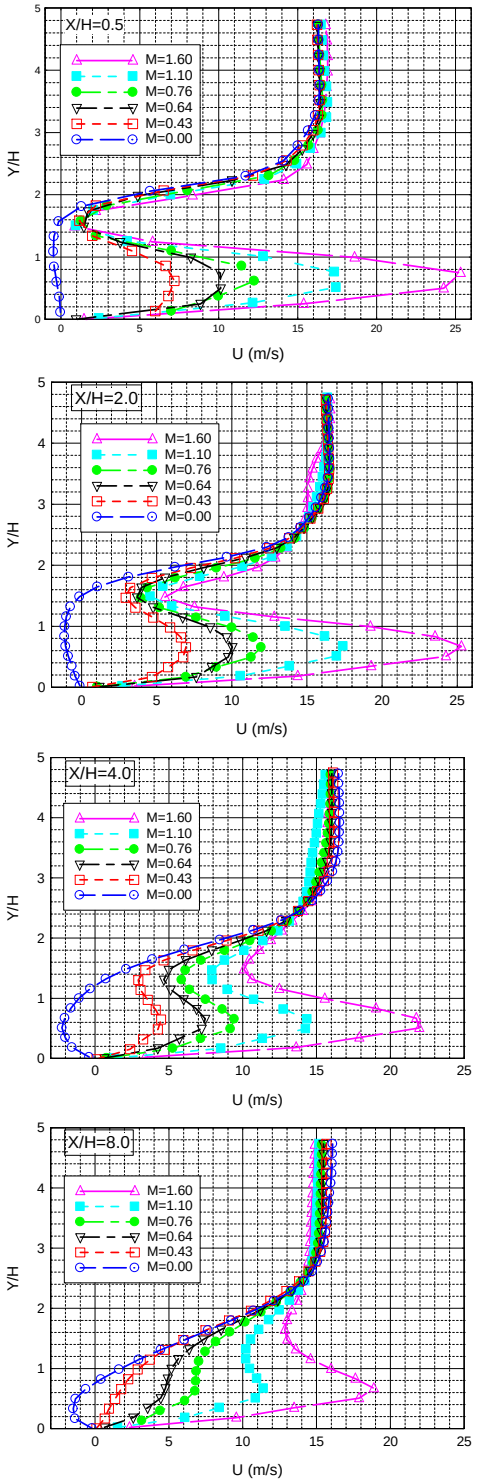

Fig. 5: Streamwise velocity profiles with various blow ratios at different distances after the exits.

B. STEREO PIV MEASUREMENT RESULTS AT DIFFERENT DOWNSTREAM LOCATIONS

B-1. The effect of blow ratios

Fig. 6 shows the three-dimensional velocity vectors and the contour of the streamwise velocity values for both the test cases without lands and with lands in the breakout region at a blow ratio of 0.43. In general, it can be seen clearly that coolant flows with a jet shape coming out from the breakouts. In the last two cross planes a4 and a5 near the end shown in Fig. 6, the jet shape disappears, which indicates the mixing process is well done. For the case without lands, as shown in Fig. 6(a), there are inverse flows shown at two sides of the measurement plane a1 and a2. Because there exists low-speed 'vacuum' regions between slot jet flows under the lip step as one might expect. The low pressure in the vacuum region results in the suction effect which induces the inverse vectors. For the case with lands as shown in Fig. 6(b), no inverse flow vectors were found. But at a first glance, very similar flow distribution is found in the slot flow valley as that without lands. Small velocity values, even negative values, can be found near the top surface of the land due to the flow separation at the lip region. More detailed flow comparison will be revealed in the next section.

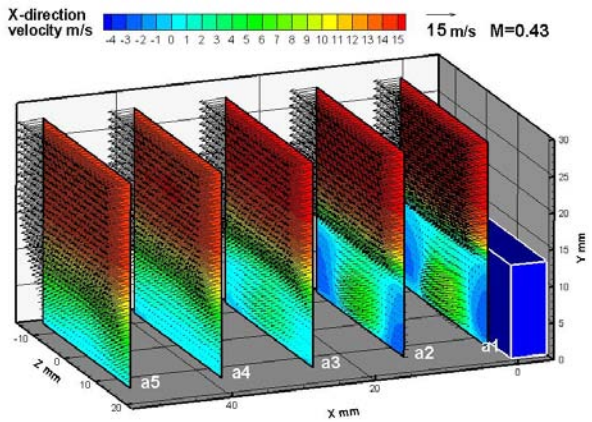

(a). without land

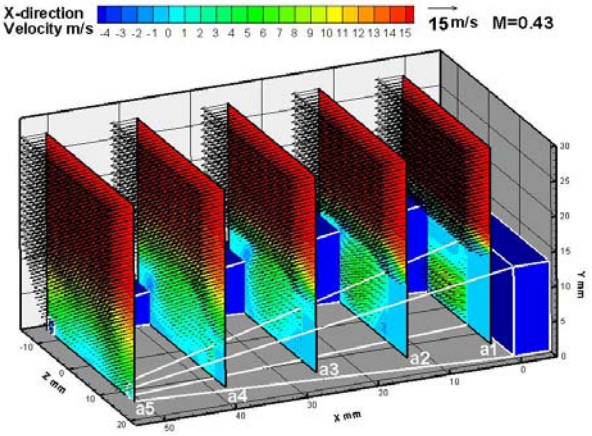

(b). with land.

Fig. 6: Stereoscopic PIV measurement results at blow ratio of M=0.43.

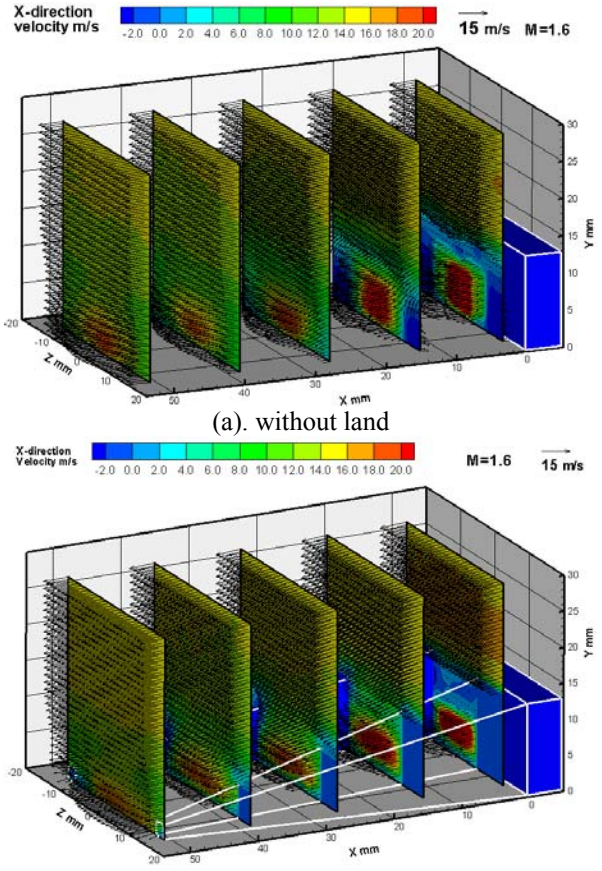

(a). without land

(b). with land.

Fig. 7: Stereoscopic PIV measurement results at blow ratio of M=1.6

Fig. 7 shows the three-dimensional velocity vectors and the contour of the streamwise velocity values at a higher blow ratio of M=1.6. The jet shapes of coolant flow are much easier to observe compared with the test case at low blow ratios. The jet shapes of the cooling stream are kept until very end cross plane (X/H=8). The longer jet shape of the cooling stream indicates better coverage over the protected surface, i.e., cooling effectiveness. The high-speed cooling jet regions for the case with lands were found to be wider than those without lands. It indicates that the existence of lands would be helpful to guild the cooling streams moving to protect the surface in the downstream of the breakout exit.

Based on the Stereo PIV measurement results, the streamwise vorticity distributions of the cooling jet streams can be obtained. Fig. 8 shows the ensemble-averaged vorticity distributions in three typical cross planes at both low and high blow ratios. The streamwise vorticity is known to greatly enhance mixing in shear layers [10]. Basically, there always appear paired vortex structures with adverse signs of the vorticity value which means an adverse rotational direction. The vortices tend to be stronger in the very end cross-plane for the case with lands because of the development of the mixing process. The measurement results revealed that the unsteady vortex structures would originate at the upper wall of the breakout, which agrees with the results found by Medic and Durbin [3]. This vortex flow pattern is kept in the downstream flow. For lower blow ratios, the entrainment of mainstream flow tends to drive the cooling jet stream in the valley to escape from the valley to form vortex structure around the edge of lands. This phenomenon does not happen when the velocity of cooling jet stream is higher than mainstream flow (M=1.6), as shown in Fig. 8 (b), because the momentum of the cooling stream is higher than that of the mainstream flow. In conclusion, the interaction between the mainstream flow and cooling stream is very strong. The blow ratios have significant effects on the vortex structures generated in the mixing process.

As shown in Fig.9 and Fig.10, for the case without lands, the flow pattern in the side region is totally different for a low and a high blow ratio at different cross planes. At a low blow ratio, the mainstream entrainment produces updraft flow in the side regions, which will allow the coolant flow to cover this region easier. Therefore higher cooling effectiveness could be expected. But at high blow ratios, since the coolant flow has more momentum, the jet flow entrainment produces downdraft flow in the side regions. This behavior will bring more mainstream flow into the side regions hence it may result in lower cooling effectiveness.

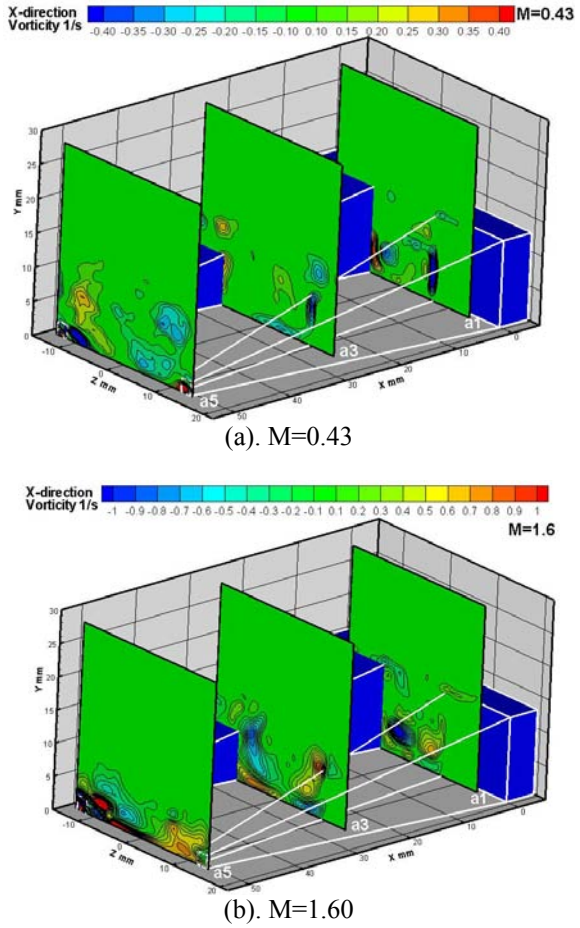

(a). M=0.43

(b). M=1.60

Fig. 8: Averaged streamwise vorticity contour with varied blow ratios for the cases with lands

B-2. The effect of the existence of lands

In order to show the effect of the existence of lands, Fig. 9 shows a direct comparison of the land effect in four lateral cross planes at different distances downstream of the breakout for both low and high blow ratios. For the low blow ratio of M=0.43 and high blow ratio of M=1.6, the existence of lands suppresses the expanding motion in the lateral direction of the coolant flow. As mentioned before, the restriction of lands makes the high-speed region of coolant flow a little bit wider than that without lands. As shown in Fig. 9, for the case without lands at a low blow ratio, the coolant flow spreads laterally and turns up mixing with the mainstream flow at upper level in the side regions. On the other hand, the updraft coolant flow in the mid-span region mixes with the mainstream flow above the upper wall of the exit before X/H=4. After X/H=4 the mainstream flow comes down drastically in the whole region and mixes with coolant jet flow. However, for the case with lands, since the lateral flow has been restricted, the coolant flow tends to climb the side wall of lands and reach the top surfaces of lands to mix with the mainstream flow. In the slot region, the updraft coolant flow mixes with the mainstream flow above the upper wall of the exit before X/H=4. After X/H=4 the mainstream flow comes down and mixes with the coolant flow. Compared to the case without lands, the streamwise velocity contour shows less high-speed region in the cross planes downstream. It indicates the existence of lands limits the invasion of mainstream flow to some extent.

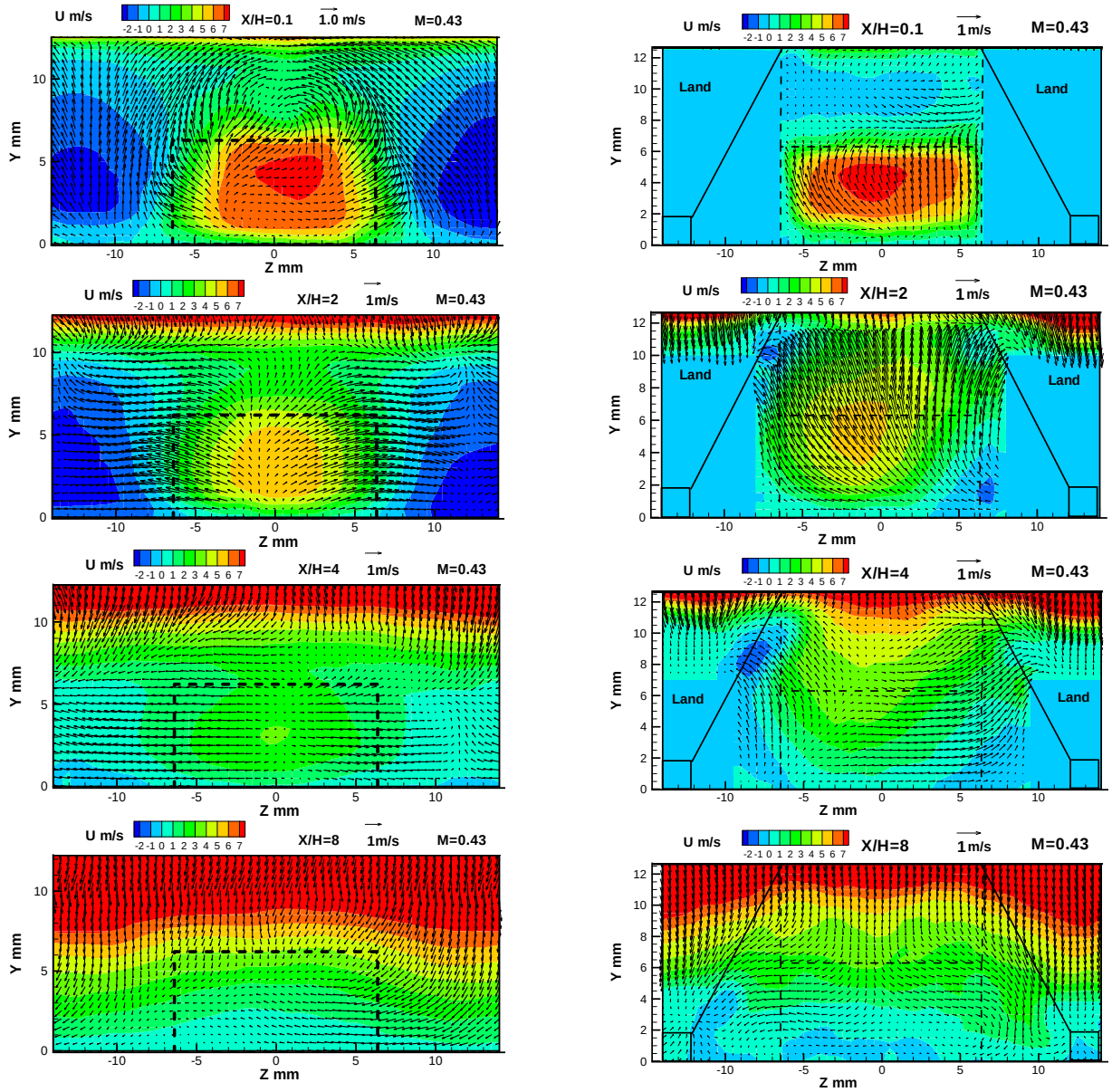

Fig. 9: Flow field comparisons at different distance downstream

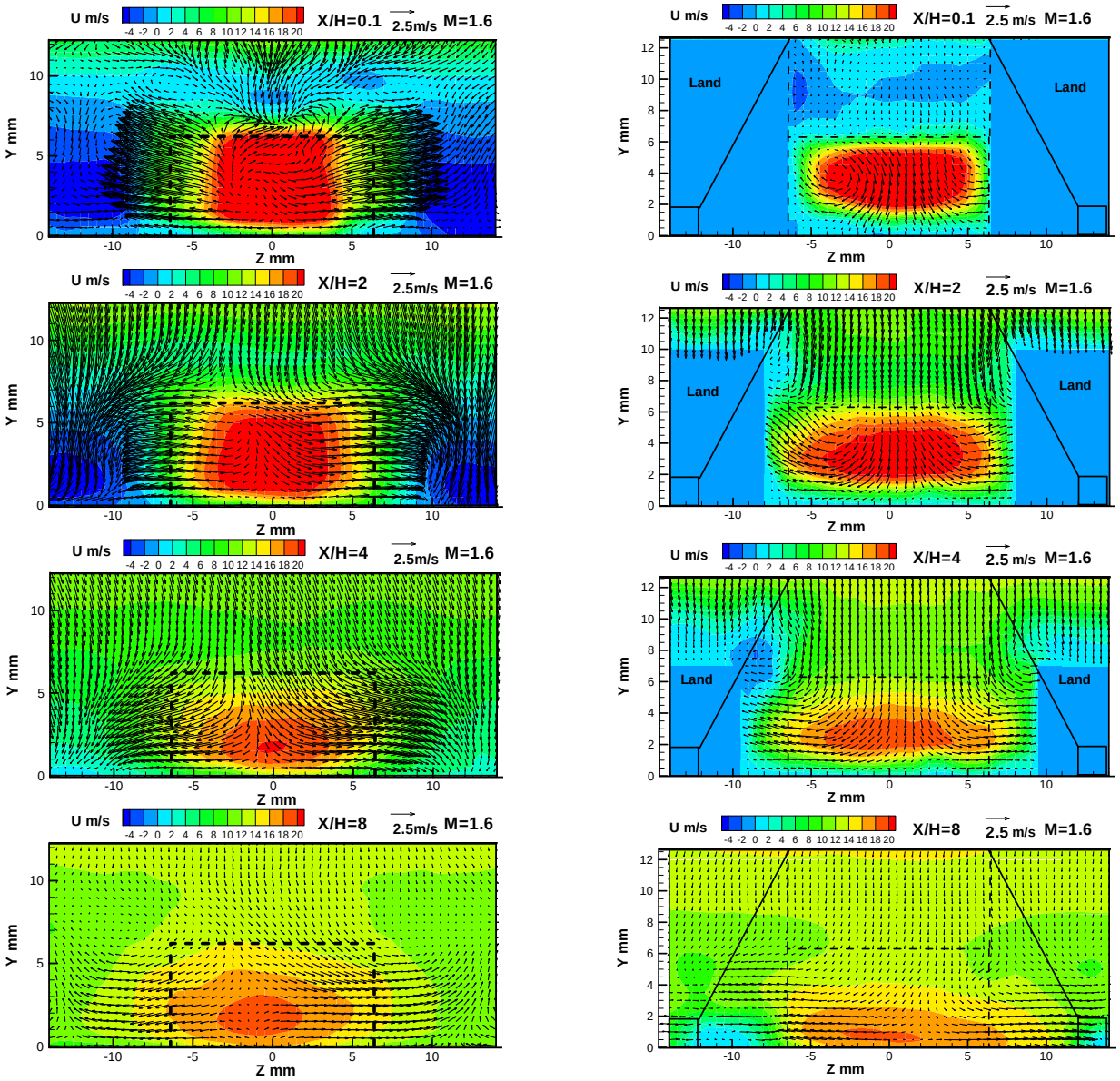

Fig. 10: Flow field comparisons at different distance downstream

As shown in Fig. 10, for the case without lands at a high blow ratio, on one hand the coolant flow spreads laterally and mixes with the downdraft mainstream flow at lower level close to the bottom in the side regions, which is different from the findings at low blow ratio. On the other hand, the mainstream flow suddenly comes down near the exit and mixes with the coolant flow. This downdraft flow pattern is kept until the end cross plane. For the case with lands, since the lateral flow has been restricted, the velocity vectors are much shorter than those for the case without lands and the coolant flow tends to form vortices at both sides of the exit. The vorticity contour has been shown in Fig. 8. The slot flow tries to climb the wall of lands and meets the down draft flow around the corner edges of the lands. High vortcity contours were also found in this region.

According to the flow features revealed in the Stereo PIV measurements, the three-dimensional flow structure was reconstructed schematically. Fig. 11(a) shows the flow structure in the trailing edge region at low blow ratios. It can be shown that the mainstream flow tends to mix with the coolant flow downstream of the slot. The coolant flow in the slot tends to climbing up around the edges of lands due to the entrainment of high-momentum mainstream flow. Fig. 11(b) shows the flow structure in the trailing edge region at high blow ratios. The mainstream flow is entrained by the high-momentum coolant flow, which results in the downward flow pattern of the mainstream flow. But the high-momentum coolant flow keeps a laminar boundary layer flow above the surface of the slot. The mainstream flow near the edges of lands tends to flowing downward around the edges due to the entrainment.

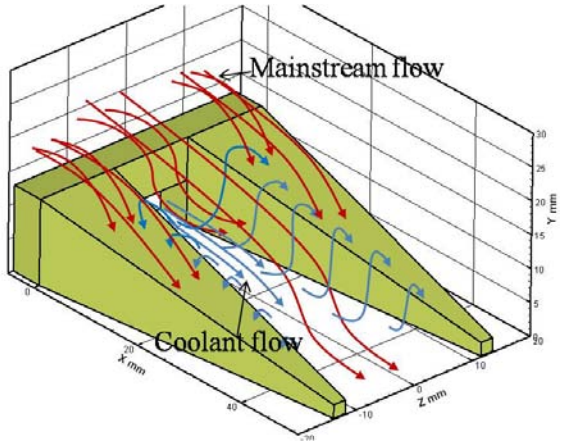

(a). Flow structure at a low blow ratio

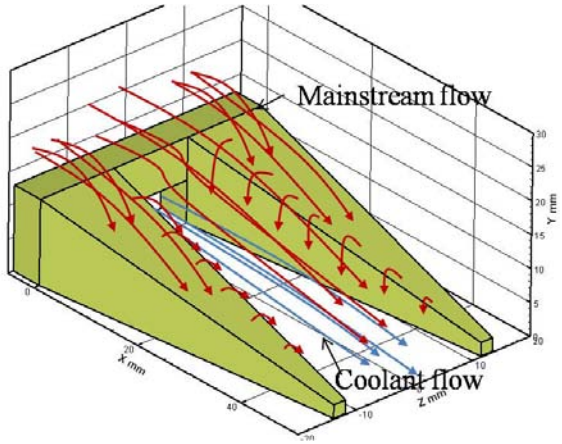

(b). Flow structure at a high blow ratio

Fig. 11: Illustration of flow structures in the trailing edge of a turbine blade

C. PSP MEASUREMENT RESULTS

Fig. 12 shows some typical PSP measurement results in the terms of adiabatic cooling effectiveness distributions on the protected surface at the downsteam of the breakout exit at different blow ratios. It can be seen clearly that, as the cooling streams were blow out from the breakout slots, high cooling effectiveness was found to concentrate in the region downstream the breakout, and low cooling effectiveness region would be on the land region, as expected. Effectiveness magnitudes close to the breakout exit are about 1.0, which indicates that the mainstream flow is not able to reach to the protected surface in those regions.

As the blowing ratio increases, the cooling effectiveness over the protected surface was found to become better and better since more cooling streams would cover the protected area in the cutback region better, as expected. It should be noted that cooling effectiveness distribution at M=1.1 shows a slightly different trend for the regions close to the ends of the lands. This characteristic distribution was also observed by Joo and Durbin [9] using large eddy simulation. This may be attributed to the enhanced mixing at the centerline near the end due to the strong vortex shedding as well as due to the relatively weak mixing in the region near lands. This result supports findings by Holloway [7] that effect of vortex shedding on the mixing process is most intensive for blowing ratios around unity. The cooling stream covers most area at the highest blowing ratio of M=1.6 as expected in the present study. However, the film cooling effectiveness distribution on the land decreases drastically with increasing blowing ratios. This can be explained by flow characteristics in the cutback region and lands as shown in Fig. 11. At a low blowing ratio of M=0.4, the cooling stream in the slot tends to climbing up around the edges of lands due to the entrainment induced by the high-momentum mainstream flow. As shown in Fig. 11(b), the mainstream flow is entrained by the high-momentum cooling streams at a high blowing ratio, which resulted in the downward flow pattern of the mainstream flow. But the high-momentum coolant flow keeps a laminar boundary layer flow above the surface of the slot. The mainstream flow near edges of lands tends to slid down around the edges due to the entrainment resulting in a swirling motion of the flow. Therefore it is easier for the cooling streams to mix with the mainstream air flow due to the entrainment and create more coverage in the lateral direction on the land at relatively low blowing ratios. But at high blowing ratios (M=1.1 and M=1.6), it seems that the high-momentum coolant flow restricts the lateral flow motion around the lands, hence the coolant flow is not able to cover the top surfaces of lands easily. Numerical simulations conducted by Chen et al. [12] also showed very high effectiveness in the cutback slots with almost no heat flux across the slots for M>1.3.

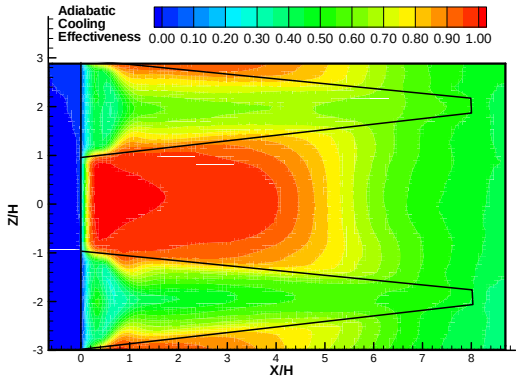

(a). M=0.40

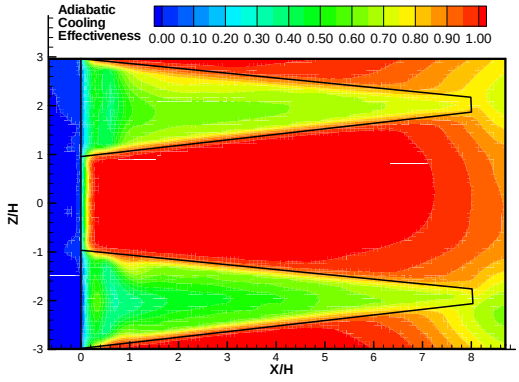

(b). M=0.80

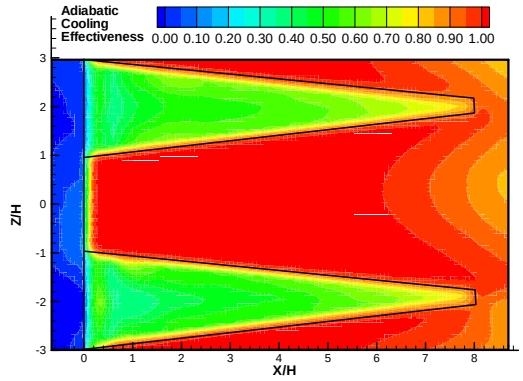

(c). M=0.11

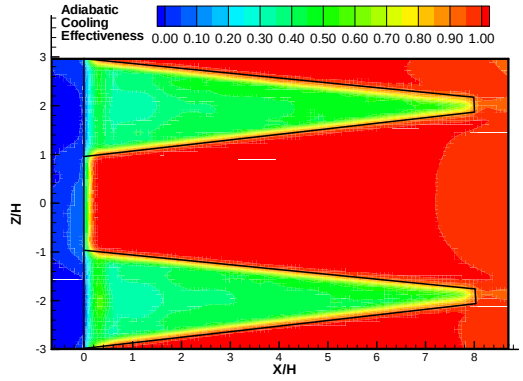

(d). M=0.16

Fig. 12: Adiabatic cooling effectiveness on the trailing edge for different blowing ratios.

CONCLUDING REMARKS

An experimental study was conducted to investigate the evolutions of the vortex and flow structures in slot wall jets pertinent to trailing edge cooling of turbine blades. A Stereo-PIV system was used to conduct detailed flow measurements in the slot wall jet flows downstream of the breakout exit of a typical gas turbine blade. Pressure sensitive paint (PSP) technique was used in the present study to measure the adiabatic cooling effectiveness distribution over the protected surface at the downstream of the breakout exit. The effects of the blow ratio of the cooling stream on the flow mixing between the main stream and cooling jet streams and the resultant adiabatic film cooling effectiveness distributions over the protected surface were investigated in great detail. The detailed flow field measurements are correlated with the adiabatic cooling effectiveness maps to elucidate underlying physics to provide further insight for improved cooling effectiveness in order to protect the critical portions of turbine blades from the harsh ambient conditions

ACKNOWLEDGMENTS

The authors are grateful to Mr. Bill Rickard of Iowa State University for his help in conducting the experiments. The support of National Science Foundation CAREER program under award number of CTS-0545918 is gratefully acknowledged

REFERENCES

[1] Holloway, S. D., Leylek, J. H., and Buck, F. A., "Pressure-Side Bleed Film Cooling: Part 1, Steady Framework for Experimental and Computational Results," ASME Paper No. GT-2002-30471, 2002.

[2] Holloway, S. D., Leylek, J. H., and Buck, F. A., "Pressure-Side Bleed Film Cooling: Part 2, Unsteady Framework for Experimental and Computational Results," ASME Paper No. GT-2002-30472, 2002.

[3] Medic, G., Durbin, P. A., "Unsteady Effects on Trailing Edge Cooling," ASME J. Heat Transfer, 127, 2005, pp. 388-392.

[4] Taslim, M. E., Spring, S. D., and mehlman, b. P., "An Experimental Investigation of Film Cooling Effectiveness for Slots of Various Exit Geometries," J. Thermophys. Heat Transfer, vol.6, No.2, 1992, pp. 302-307.

[5] Brundage, A. L., Plesniak, M. W., Lawless, P. B., and Ramadhyani, S., "Experimental Investigation of Airfoil Trailing Edge Heat Transfer and Aerodynamic Losses," Experimental Thermal and Fluid Secience, Vol.31, 2007, pp. 249-260.

[6] Cakan, M., Taslim, M. E., "Experimental and Numerical Study of Mass/Heat Transfer on an Airfoil Trailing-Edge Slots and Lands", ASME J. Turbomach., vol. 129, 2007, pp. 281-293.

[7] Choi, J. H., Mhetras, S., Han, J. C., Lau, S. C., and Rudolph, R., "Film Cooling and Heat Transfer on Two Cutback Trailing Edge Models With Internal Perforated Blockages", ASME J. Heat Transfer, Vol.130, 2008, 012201:1-13. doi:10.1115/1.2780174

[8] Martini, P., Schulz, A., and Bauer, H.-J., "Film Cooling Effectiveness and Heat Transfer on the Trailing Edge Cutback of Gas Trubine Airfoils With Vairous Internal Cooling Designs", ASME J. Turbomach., Vol.128, 2006, pp. 196-205.

[9] Ahn J, Mhetras, S. Ha KC., Film-Cooling Effectiveness on a Gas Turbine Blade Tip Using Pressure-Sensitive Paint, Journal of Heat Transfer, Vol. 127 No. 521, 2005.

[10] Suryanarayanan A., Mhetras S. P., Schobeiri, M. T. and Han J. C., "Film-Cooling Effectiveness on a Rotating Blade Platform", J. Turbomach. Vol. 131, No. 1, 011014, 2009. doi:10.1115/1.2752184.

[11] Yang, Z. "Experimental Investigations on Complex Vortex Flows Using Advanced Flow Diagnostic Techniques", Ph. D. thesis, Iowa State University, 2009.

[12] Chen, S. P., Li, P. W., Chyu, M. K., Cunha, F. J., and Abdel-Messeh, W., "Heat Transfer in an Airfoil Trailing Edge Configuration With Shaped Pedestals Mounted Internal Cooling Channel and Pressure Side Cutback,", ASME Paper No. GT2006-91019, 2006.